RUSSIAN JOURNAL OF EARTH SCIENCES
vol. 20, 2, 2020, doi: 10.2205/2020ES000711

Tidal internal waves in the Bransfield Strait, Antarctica

E. E. Khimchenko[1], *D. I. Frey*[1],
E. G. Morozov[1]

Shirshov Institute of Oceanology RAS, Moscow, Russia

Abstract. Observations of tidal internal waves in the Bransfield Strait, Antarctica, are analyzed. The measurements were carried out for 14 days on a moored station equipped with five autonomous temperature and pressure sensors. Vertical displacements of temperature revealed that strong internal vertical oscillations up to 30–40 m are caused by the diurnal internal tide. The waves are forced due to the interaction of the barotropic tide with the bottom topography. The velocity ellipses of the barotropic tidal currents were estimated using the global tidal model.

This is the e-book version of the article, published in Russian Journal of Earth Sciences (doi:10.2205/2020ES000711). It is generated from the original source file using LaTeX's **ebook.cls** class.

Introduction

Tidal internal waves exist everywhere in the World Ocean. The most common mechanism for their generation is associated with the interaction of the currents of the barotropic tide with the slopes of bottom topography, which leads to the excitation of internal waves with heights of several tens, and in some cases, hundreds of meters [*Morozov,* 1995, 2018]. Propagation of internal tides often leads to the generation of large-amplitude high-frequency internal waves [*Sabinin et al.,* 2004; *Sabinin and Serebryany,* 2005, 2007]. However, observations of internal waves at high latitudes are rare. The principal difference between semidiurnal internal tides existing in the high latitude regions is the location of measurements either north or south of the critical latitude $74^{\circ}30'$ [*Konyaev,* 2000; *Levine et al.,* 1985; *Marchenko and Morozov,* 2016; *Marchenko et al.,* 2010; *Morozov and Pisarev,* 2002; *Morozov et al.,* 2003a, 2008; *Pisarev,* 1996]. Internal tides in the straits are generally stronger than in the open ocean because currents of the barotropic tide are intensified in the straits. Steep bottom topography at the coasts of straits facilitates intense generation of internal tides [*Morozov et al.,* 2003b, 2017, 2019]. Field measure-

ments in the Antarctic region are scarce. The most studied region of the Antarctic is the Drake Passage where field measurements have been continuing since 1975 [e.g., *Heywood et al.*, 2007; *Nowlin et al.*, 1982]. A review of tidal observations around the Antarctic coastline up to 1980 is presented in [*Lutjeharms et al.*, 1985] and the information about relatively recent studies could be found in [*Dragani et al.*, 2004]. Most of the measurements have been conducted west of the Antarctic Peninsula, more often in the Bransfield Strait [*Dragani et al.*, 2004].

The goal of this investigation in January–February 2020 was to study tidal internal waves in the Bransfield Strait. We analyzed direct temperature measurements on a mooring, which was deployed at a depth of 70 m close to Nelson Island (South Shetland Islands).

Data and Methods

During cruise 79 of the R/V *Akademik Mstislav Keldysh* to the Southern Ocean in January 2020, we deployed a mooring station in the Bransfield Strait at a depth of 70 m. The mooring was set close to Nelson Island (South Shetland Islands, Antarctica) in the northeastern part of the Bransfield Strait at coordinates 62°21.368′

S, 58°49.352′ W. The moored buoy was equipped with four Starmon Mini temperature sensors, and a DST TD pressure and temperature sensor of the Starr-Oddi Company. The time sampling of measurements was 30 s and 1 min, respectively. The sensors were initially set at depths 16, 26, 36, 46, and 56 m. Continuous recording of temperature was carried out for 14 days from 20 January to 3 February 2020. The research area, location of mooring, and bathymetry are shown in Figure 1.

The record of the pressure sensor located at a depth of 16 m showed that during the entire time of recording, the moored buoy has been deepening periodically relatively to its initial vertical position (from 0.5 to 18 m). These oscillations of mooring were caused by tidal currents and mean currents in the strait. Thus, measurements at each sensor were recorded at different depths, but the pressure sensor made possible estimating the depths of each measurement so that fluctuations of isotherms were revealed.

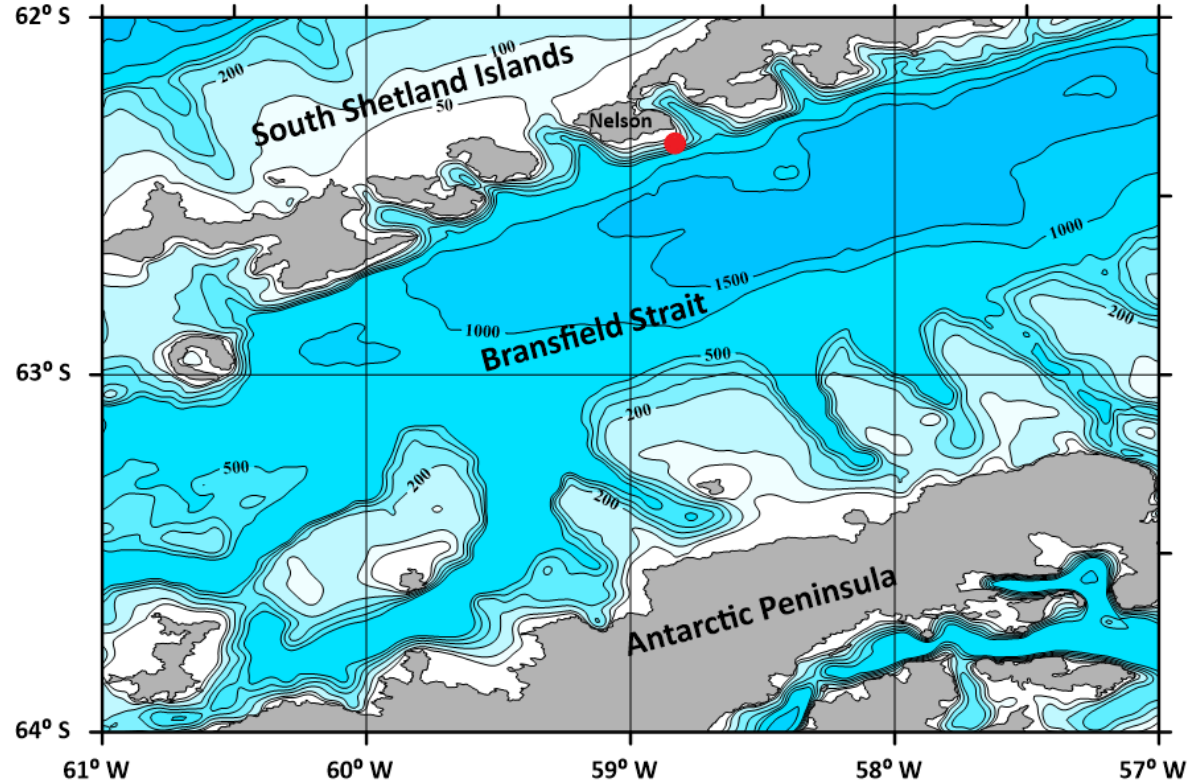

Figure 1. Bathymetry of the study region and location of the mooring (marked with a red dot).

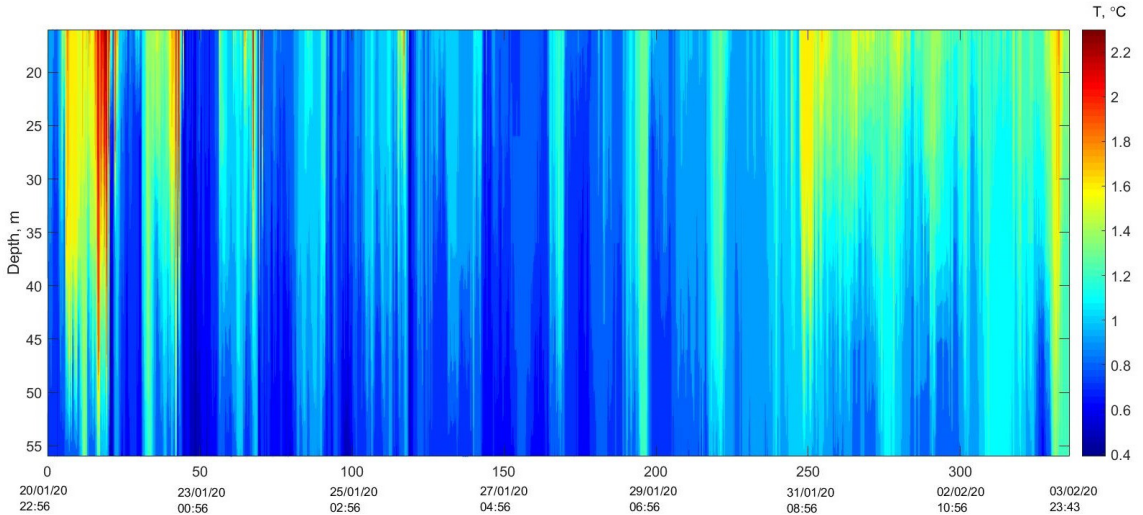

Figure 2. Time variations of the displacement of isotherms during measurements.

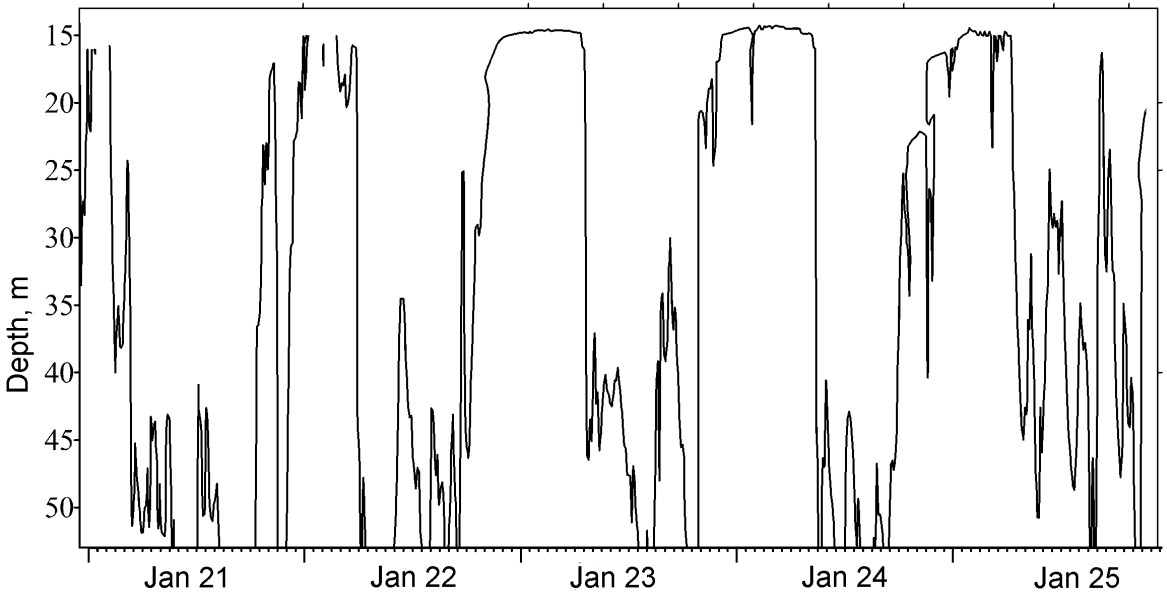

Figure 3. Time variation of the 0.9°C isotherm from 21 January to 25 January 2020.

Results and Discussion

The color graph in Figure 2 presents displacements of isotherms from 20 January to 3 February 2020. Displacement of the 0.9°C isotherm, which is the most representative, is shown in Figure 3. The most intense vertical displacements of isotherms were identified in the middle part of the observation period. Displacements of isotherms indicate that the oscillations with a diurnal frequency close to 24 h dominate. These oscillations were caused by the propagation of diurnal internal waves. Note that the critical latitude for the 24 h diurnal internal waves is 30°. Hence, the diurnal period of internal tides recorded in our experiment is related to the forced internal waves on the slope of Nelson Island. Such waves cannot propagate further as free internal waves. They exist only over the sloping bottom of the shelf region. The heights of fluctuations with a 24 h period reached 40 m. The New Moon was on 25 January; hence, our measurements were performed almost during the spring tide, which caused intense tidal internal waves. Less intense oscillations in the range between the semidiurnal and inertial periods were identified only at the end of the time series. The local inertial period in the study site is 13.5 h.

Spectral analysis of the time series of the displacement of the 0.9°C isotherm has been performed from the time period from 20 to 27 January (Figure 4). The spectrum demonstrates the existence of a clear peak at the diurnal 24 h period that apparently corresponds to the diurnal tidal period. A peak at the sub-inertial period appears only at the spectrum of average temperature fluctuations which is not reliable.

It is known that the M_2 component of the barotropic tide with a period 12.4 h is the most energetic one in the major part of the World Ocean. However, in the Antarctic region of the Southern Ocean, tides are of irregular semidiurnal and mixed diurnal and semidiurnal character, moreover, the diurnal component is maximum in the summer season [*Foldvik et al.*, 1985]. It is likely that we recorded this intensification of the diurnal tide component during the Antarctic summer. At each point of the sea, the variations in the tides depend on the geographical conditions, i.e., on the shape of the coastline, peculiarities of the bottom topography, and the presence of islands. It was shown in [*Lim*, 2014] based on numerical modeling that the M_2 and K_1 tidal waves arriving from the Southern Ocean and the Weddell Sea slow down as they propagate into the Bransfield Strait where the water depths are relatively

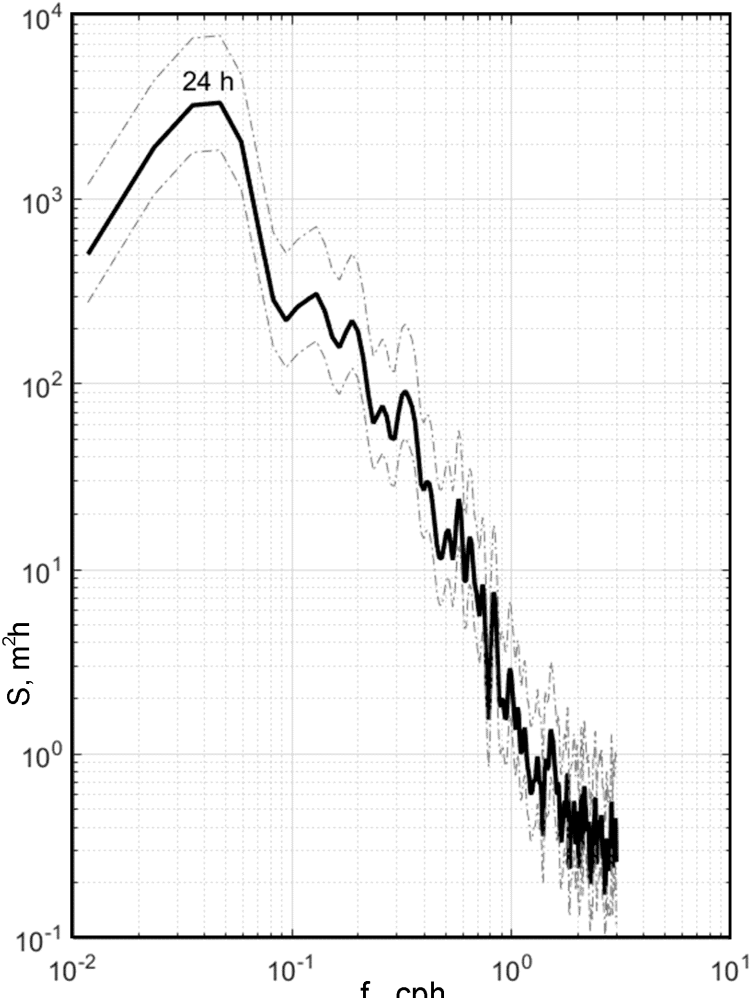

Figure 4. Frequency spectrum of vertical displacements of isotherm 0.9°C. Dashed lines show the 95% confidence interval.

shallower. The diurnal tidal amplitudes increase gradually from King George Island (which is close to Nelson Island) to the Antarctic Peninsula.

The velocity of barotropic tidal currents and sea level elevations in the study site were calculated from satellite altimetry measurements using the global tidal model TPXO9.0 of Oregon State University (USA) [*Egbert and Erofeeva,* 2002]. The earlier version of this model was used for the calculation of tides over the continental shelf west of the Antarctic Peninsula. The estimates of the observed and simulated tides were in a good agreement [*Klinck,* 1995]. Sea level elevation occurs both with the semidiurnal and diurnal periods. The heights of the diurnal tidal waves are more intense and reach 1–1.5 m (Figure 5a) with a maximum on 25–27 January, which coincides with the spring tide. Progressive vector diagrams were constructed for the first 120 h of observations based on the calculated barotropic tidal flow velocities (Figure 5b). It can be seen that during the calculation period, five cycles of rotation of the ellipses rotate clockwise with a period of 24 h and the ellipses a period of 12 h rotate anticlockwise (Figure 5b). Such behavior of counterclockwise rotation of semidiurnal tides and clockwise rotation of diurnal tides was observed in the Drake Passage in [*Nowlin et al.,* 1982].

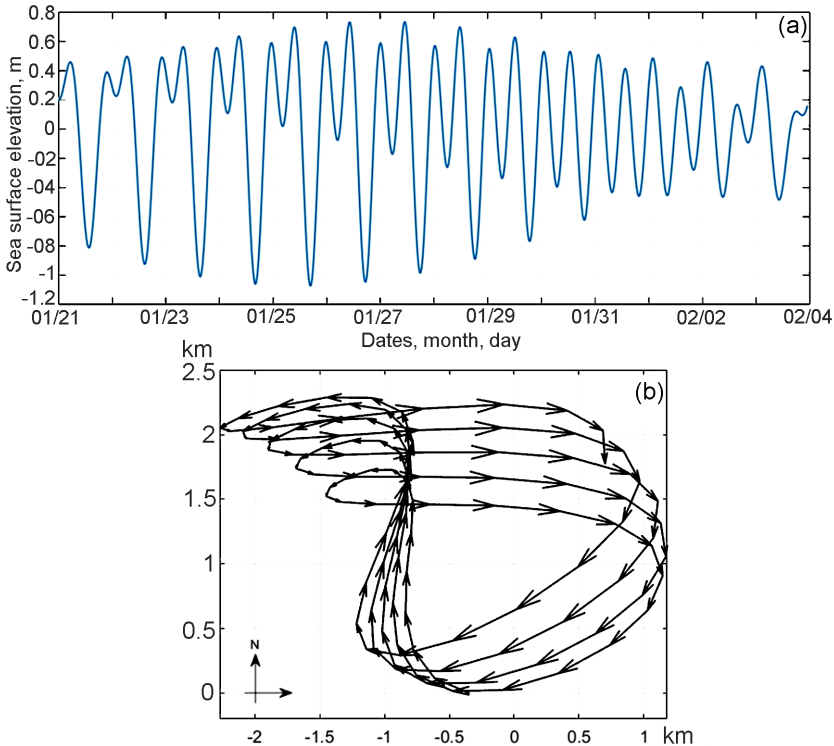

Figure 5. Sea surface elevation at the study site during the period of observations in January–February 2020 (a); progressive vector diagrams of tidal ellipses based on the model TPXO9.0 on 21–25 January (b).

Conclusions

We analyzed fluctuations of isotherms measured on a mooring deployed at a depth of 70 m in the Bransfield Strait, Antarctica, carried out during 14 days in January–February 2020. It was shown that tidal internal waves of the diurnal period with heights of 30–40 m were observed in the study site. Spectral analysis of vertical displacements of the 0.9°C isotherm showed a clear peak at a period of 24 h. It is known that the tides in the Bransfield Strait are mostly mixed diurnal and semidiurnal, but during the Antarctic summer, diurnal tide component may intensify. Using the global tidal model TPXO9.0 it was found that tidal ellipses rotate clockwise with a period of 24 h and anticlockwise with a period of 12 h.

Acknowledgments. This research was performed in the framework of the state assignment of Russia (theme No. 0128-2019-0008). The work was supported by the Russian Foundation for Basic Research (grant nos. 20-08-000246, 19-05-00715, and 19-57-60001).

References

Dragani, W. C., M. R. Drabble, E. E. D'Onofrio, C. A. Mazio (2004) , Propagation and amplification of tide at the Bransfield and Gerlache straits, northwestern Antarctic Peninsula, *Polar Geosci.*, *17*, p. 156–170.

Egbert, G. D., S. Y. Erofeeva (2002) , Efficient inverse modeling of barotropic ocean tides, *Journal of Atmospheric and Oceanic Technology*, *19*, no. 2, p. 183–204, **Crossref**

Foldvik, A., T. Kvinge, T. Tørresen (1985) , Bottom currents near the continental shelf break in the Weddell Sea, *Antarctic Research Series*, *43*, p. 21–34.

Heywood, K. J., J. L. Collins, C. W. Hughes, I. Vassie (2007) , On the detectability of internal tides in Drake Passage, *Deep-Sea Res.*, *54*, no. 1, p. 1972–1984, **Crossref**

Klinck, J. M. (1995) , Palmer LTER: comparison between a global tide model and observed tides at Palmer Station, *Antarc. J. U. S.*, *30*, p. 263–264.

Konyaev, K. V. (2000) , Internal tide at the critical latitude, *Izvestia Atmos. Oceanic Phys.*, *36*, p. 363–375.

Levine, M. D., C. A. Paulson, J. H. Morison (1985) , Internal waves in the Arctic Ocean: Comparison with lower-latitude observations, *J. Phys. Ocean.*, *15*, no. 6, p. 800–809, **Crossref**

Lim, C. H. (2014) , Modelling waves and currents in Potter Cove, King George Island, Antarctica, PhD thesis, Carl von Ossietzky University, Oldenburg, Germany.

Lutjeharms, J. R. E., et al. (1985) , Tidal measurements along the Antarctic coastline, *Oceanology of the Antarctic Continental*

Shelf, *43*, p. 273–289.

Marchenko, A. V., E. G. Morozov (2016) , Surface manifestations of the waves in the ocean covered with ice, *Russian J. Earth Sciences*, *16*, no. 1, p. ES1001, **Crossref**

Marchenko, A. V., E. G. Morozov, S. V. Muzylev, A. S. Shestov (2010) , Interaction of short internal waves with the ice cover in an Arctic fjord, *Oceanology*, *50*, no. 1, p. 18–27, **Crossref**

Morozov, E. G. (1995) , Semidiurnal internal wave global field, *Deep Sea Research*, *42*, no. 1, p. 135–148, **Crossref**

Morozov, E. G. (2018) , *Oceanic Internal Tides: Observations, Analysis and Modeling: A Global View*, Springer, **Crossref**

Morozov, E. G., S. V. Pisarev (2002) , Internal tides at the Arctic latitudes (numerical experiments), *Oceanology*, *42*, p. 165–173.

Morozov, E. G., S. V. Pisarev, V. G. Neiman, S. Y. Erofeeva (2003a) , Internal tidal waves in the Barents Sea, *Doklady Earth Sciencies*, *393*, no. 8, p. 1124–1126.

Morozov, E. G., G. Parrilla-Barrera, M. G. Velarde, A. D. Scherbinin (2003b) , The Straits of Gibraltar and Kara Gates: A comparison of internal tides, *Oceanologica Acta*, *26*, no. 3, p. 231–241, **Crossref**

Morozov, E. G., V. T. Paka, V. V. Bakhanov (2008) , Strong internal tides in the Kara Gates Strait, *Geophysical Research Letters*, *35*, p. L16603, **Crossref**

Morozov, E. G., I. E. Kozlov, S. A. Shchuka, D. I. Frey (2017) , Internal tide in the Kara Gates Strait, *Oceanology*, *57*, no. 1, p. 8–18, **Crossref**

Morozov, E. G., A. V. Marchenko, K. V. Filchuk, et al. (2019) , Sea ice evolution and internal wave generation due to a tidal

jet in a frozen sea, *Applied Ocean Research*, *87*, p. 179–191, **Crossref**

Nowlin, W. D. Jr., J. S. Bottero, R. D. Pillsbury (1982) , Observations of the principal tidal currents at Drake Passage, *Journal of Geophysical Research: Oceans*, *87*, no. C8, p. 5752–5770, **Crossref**

Pisarev, S. V. (1996) , Low-frequency internal waves near the shelf edge of the Arctic basin, *Oceanology*, *36*, no. 6, p. 771–778.

Sabinin, K., A. Serebryanyi (2005) , Intense short-period internal waves in the ocean, *Journal of Marine Research*, *63*, no. 1, p. 227–261, **Crossref**

Sabinin, K. D., A. N. Serebryanyi (2007) , "Hot spots" in the field of internal waves in the ocean, *Acoustical Physics*, *53*, no. 3, p. 357–380, **Crossref**

Sabinin, K. D., A. N. Serebryanyi, A. A. Nazarov (2004) , Intensive internal waves in the World Ocean, *Oceanology*, *44*, no. 6, p. 753–758.